Ultralow reverse leakage current in AlGaN/GaN lateral Schottky barrier diodes grown on bulk GaN substrate

2016 Appl. Phys. Express 9 031001

(http://iopscience.iop.org/1882-0786/9/3/031001)

Applied Physics Express **9**, 031001 (2016)
http://doi.org/10.7567/APEX.9.031001

Ultralow reverse leakage current in AlGaN/GaN lateral Schottky barrier diodes grown on bulk GaN substrate

Xing Lu[1*], Chao Liu[2], Huaxing Jiang[2], Xinbo Zou[2], Anping Zhang[1], and Kei May Lau[2]

[1]*State Key Laboratory of Electrical Insulation and Power Equipment, School of Electrical Engineering, Xi'an Jiaotong University, Xi'an 710049, China*
[2]*Department of Electronic and Computer Engineering, Hong Kong University of Science and Technology, Clear Water Bay, Kowloon, Hong Kong*

*E-mail: eexlu@connect.ust.hk

Received November 6, 2015; accepted January 12, 2016; published online January 28, 2016

We report on a study of AlGaN/GaN heterostructure lateral Schottky barrier diodes (L-SBDs) grown on a bulk GaN substrate. The L-SBDs exhibited an ultralow reverse leakage current below 10^{-6} A/cm^2 without employing any extra treatments, which was over 4 orders of magnitude lower than that of a reference device on a sapphire substrate. The superior performance was attributed to the high crystalline quality of the heterostructure achieved by homoepitaxy. The comparison also revealed that the absence of high-density trap states in the homoepitaxial L-SBD grown on the bulk GaN substrate played a key role in achieving a low reverse leakage current.

High reverse leakage current, resulting in unnecessary power consumption and reliability issues, remains a critical challenge in the development of AlGaN/GaN-based electronic devices such as lateral Schottky barrier diodes (L-SBDs) and high-electron-mobility transistors (HEMTs) for power switching and RF applications. A variety of methods have been proposed to reduce the reverse leakage current in AlGaN/GaN L-SBDs, including surface treatment,[1–6] post-gate annealing (PGA),[7,8] adding a GaN cap layer on top of the AlGaN barrier,[3,9] or employing a three-dimensional anode structure.[10] A markedly low reverse leakage current density of 10^{-5} A/cm^2 has been demonstrated in the AlGaN/GaN L-SBDs grown on sapphire substrates using a CF_4 plasma treatment.[1] However, the plasma treatments may introduce some undesirable effects on the heterostructures, such as a decrease in channel conductivity.[2,5]

It has also been reported that trap/defect-assisted tunneling and hopping through threading dislocations (TDs) could be the dominant leakage sources for an AlGaN/GaN L-SBD.[11,12] The defects and dislocations, especially TDs, are generally present at high densities in III–nitride materials heteroepitaxially grown on Si, sapphire, and SiC substrates. Huang et al.[13] have found that the high leakage current for L-SBDs grown on a sapphire substrate was mainly caused by the defect states that resulted from the TDs extending from the GaN layer to the AlGaN barrier. The use of an AlN interlayer could terminate some of the TDs to reduce the leakage current; however, it is of limited use and the leakage current density was still as high as 1.1×10^{-4} A/cm^2. In contrast, a bulk GaN substrate with low defect/dislocation density, especially low TD density, would help circumvent this problem by offering a lattice- and thermal-expansion-matched platform for the development of high-performance GaN-based devices. However, most of the studies in the literature focused on the GaN vertical SBDs or p–n diodes when employing bulk GaN substrates,[14] while results on AlGaN/GaN heterostructure L-SBDs grown on a bulk GaN substrate are very limited.[15] The AlGaN/GaN heterostructure L-SBDs are different from and more complicated than the GaN vertical SBDs and p-n diodes without heterojunctions. Moreover, the AlGaN/GaN L-SBDs featuring a two-dimensional electron gas (2DEG) channel with a large carrier concentration, a high electron mobility, and a thin lateral topology enable fast switching with low losses.[16,17]

In this work, we performed a comparative study of AlGaN/GaN L-SBDs grown on bulk n$^+$ GaN and sapphire substrates. An ultralow reverse leakage current density below 10^{-6} A/cm^2 was achieved for the L-SBD grown on the bulk GaN substrate, which was over 4 orders of magnitude lower than that on the sapphire substrate. High-resolution X-ray diffraction (XRD), atomic force microscopy (AFM), and capacitance–voltage (C–V) analysis were performed to compare the crystalline quality and trapping effects of the two heterostructures.

The AlGaN/GaN heterostructures used in this study were grown on a bulk GaN substrate and a GaN-on-sapphire template side by side in an Aixtron 2400HT metal–organic chemical vapor deposition (MOCVD) system. The epistructure, from bottom to top, consists of a 2 µm undoped GaN layer, a 1 nm AlN spacer, and a 20 nm undoped $Al_{0.3}Ga_{0.7}N$ barrier. The 270-µm-thick bulk GaN substrate is of the n-type with a resistivity of 0.04 Ω·cm and a dislocation density of ~10^7 cm^{-2}. The GaN-on-sapphire template was prepared by MOCVD with a GaN buffer thickness of 4 µm. The fabrication of L-SBDs started with mesa isolation using BCl_3/Cl_2-based inductively coupled plasma (ICP) etching. Then, Ti/Al/Ni/Au (20/150/50/80 nm) was deposited by e-beam evaporation and annealed at 850 °C for 30 s in N_2 ambient to form the Ohmic contact on the AlGaN barrier. Using the transfer length method (TLM), the Ohmic contact resistance and sheet resistance for the sample grown on the bulk GaN substrate were measured to be 0.83 Ω·mm and 540 Ω/sq, respectively, while they were 0.77 Ω·mm and 460 Ω/sq for the sample grown on the sapphire substrate. One possible reason for the different sheet resistances of the 2DEG channels could be the different strain conditions of the heterostructures grown on different substrates. Finally, a Ni/Au (20/200 nm) Schottky metal was deposited. Figure 1 shows the cross-sectional schematic of the fabricated L-SBD structure. The diameter of the circular Schottky gate was 200 µm. The distance between the Schottky gate and the ring Ohmic contact was 15 µm. No passivation was employed for the two L-SBDs.

Figure 2 shows the reverse and forward current densities of the fabricated L-SBDs grown on the bulk GaN and sapphire substrates. The L-SBD on the bulk GaN substrate exhibited a reverse leakage current density below 10^{-6} A/cm^2 at a gate bias of −35 V, while the leakage current density is above 10^{-2} A/cm^2, over 4 orders of magnitude higher, for the L-SBD grown on the sapphire substrate. The

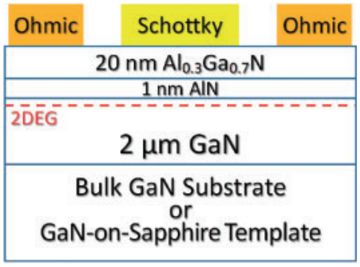

Fig. 1. Schematic cross section of the AlGaN/GaN L-SBD grown on the bulk GaN substrate or GaN-on-sapphire template.

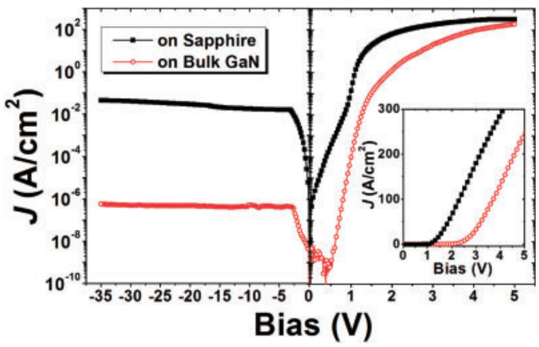

Fig. 2. Reverse and forward current densities of the AlGaN/GaN L-SBDs grown on the bulk GaN and sapphire substrates.

Table I. Benchmarks of the AlGaN/GaN L-SBDs with low reverse leakage current obtained by different approaches.

Structure	Substrate	Treatment	I_r at −35 V (A/cm^2)	Ref.
AlGaN (35 nm)/GaN	Sapphire	CF_4 plasma	$\sim 6 \times 10^{-6}$	1
GaN/AlGaN (17.5 nm)/GaN	Si	O_2 plasma	$>1 \times 10^{-4}$	3
AlGaN (25 nm)/GaN	Sapphire	PGA	$>5 \times 10^{-5}$	6
AlGaN/GaN	GaN	No	$>1 \times 10^{-4}$	14
AlGaN (20 nm)/GaN	GaN	No	$<1 \times 10^{-6}$	This work

Table II. FWHMs of the ω-rocking curves for the AlGaN/GaN structures grown on the bulk GaN and sapphire substrates (unit: arcsec).

Sample	(002) FWHM	(102) FWHM
On bulk GaN	213	291
On sapphire	390	1034

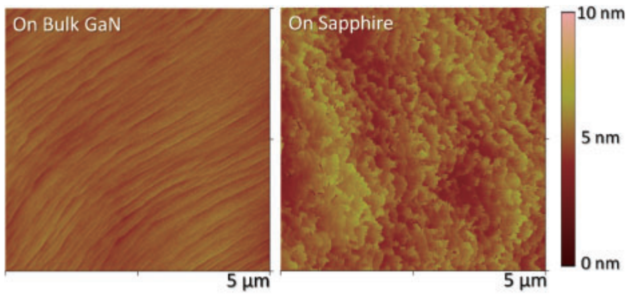

Fig. 3. AFM images of the AlGaN/GaN structures grown on the bulk GaN and sapphire substrates.

result was benchmarked with other reported AlGaN/GaN L-SBDs in the literature using different leakage reduction approaches, as listed in Table I. Our work exhibited a state-of-the-art low reverse leakage current without employing any extra treatments. The effective barrier height (ϕ_b) and ideality factor (n) of the L-SBDs can be extracted from the forward bias characteristics using the standard thermionic emission mechanisms.[11,12] In this study, the experimental values of ϕ_b/n for the L-SBDs grown on the bulk GaN and sapphire substrates are 1.25 eV/1.60 and 0.96 eV/1.92, respectively. Furthermore, a much higher turn on voltage was observed for the L-SBD grown on the bulk GaN substrate when compared with that on the sapphire substrate, as shown by the linear plot of the forward currents in the inset of Fig. 1. The high turn-on voltage of the AlGaN/GaN L-SBDs could be explained by the two-diode model,[18,19] where the heterojunction barrier between the AlGaN and GaN layers suppresses the forward current at a relatively high forward bias (1.5–2 V in this study). The Schottky contact with a sufficient ϕ_b, which controls both the depletion width and carrier transport across the interface, and a low leakage current is one of the critical factors for the realization of high-performance AlGaN/GaN-based electronic devices.

The better electrical characteristics of the L-SBD grown on the bulk GaN substrate compared with that on the sapphire substrate should be attributed to the higher crystalline quality, i.e., low defect/dislocation density, of the AlGaN/GaN structure by homoepitaxy. To evaluate the defect/dislocation density quantitatively, XRD was performed for both samples. Table II shows the full widths at half maximum (FWHMs) from the two AlGaN/GaN heterostructures. It can be clearly seen that the sample grown on the bulk GaN substrate exhibited much smaller FWHM values than that on the sapphire substrate, which indicates a better crystalline quality. The surface morphology of the two samples was investigated by AFM, as shown in Fig. 3. The AlGaN/GaN structure grown on the bulk GaN substrate showed a very smooth surface and well-aligned atomic step flow patterns, with a root-mean-square (RMS) roughness of 0.24 nm across a $5 \times 5\,\mu m^2$ scanned area. In contrast, the atomic steps are disordered for the heterostructure grown on the sapphire substrate and the RMS roughness is also larger (0.64 nm). Moreover, high-density small pits can be observed on the surface of the AlGaN/GaN structure grown on the sapphire substrate, while they did not appear for the bulk GaN substrate. The surface pits seem to be pinholes that originated from the extended dislocations to the AlGaN barrier from the buffer layer.[20,21] We consider that these high-density pinholes also give rise to the large reverse leakage current and low ϕ_b in the L-SBD grown on the sapphire substrate.

The emission of electrons via a trap state into a continuum of states associated with the presence of conductive dislocations was the dominant leakage mechanism in an AlGaN/GaN L-SBD,[11,12] which could be successfully explained by the Frenkel–Poole emission model. The current density associated with Frenkel–Poole emission is given by

$$J = CE_b \exp\left[-\frac{q(\phi_T - \sqrt{qE_b/\pi\varepsilon_0\varepsilon_s})}{kT}\right],$$

where E_b is the electric field in the semiconductor barrier, ϕ_T is the barrier height for electron emission from the trap state, and C is a constant. As shown in Fig. 4, the linear dependence of $\ln(J/E_b)$ on $\sqrt{E_b}$ is a proof of the Frenkel–Poole effect of the AlGaN/GaN L-SBDs in this study.

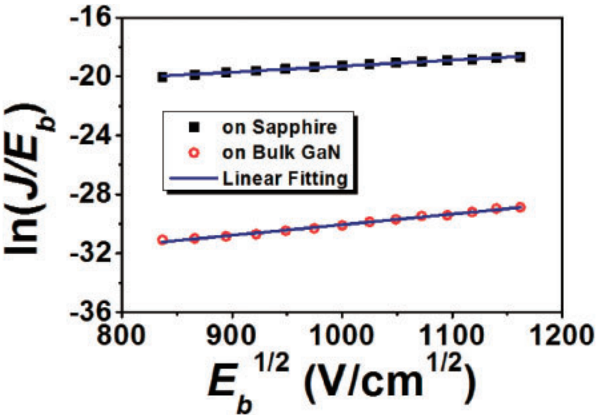

Fig. 4. Measured reverse current density (J) divided by the electric field in the AlGaN barrier (E_b) versus square root of E_b for the two L-SBDs.

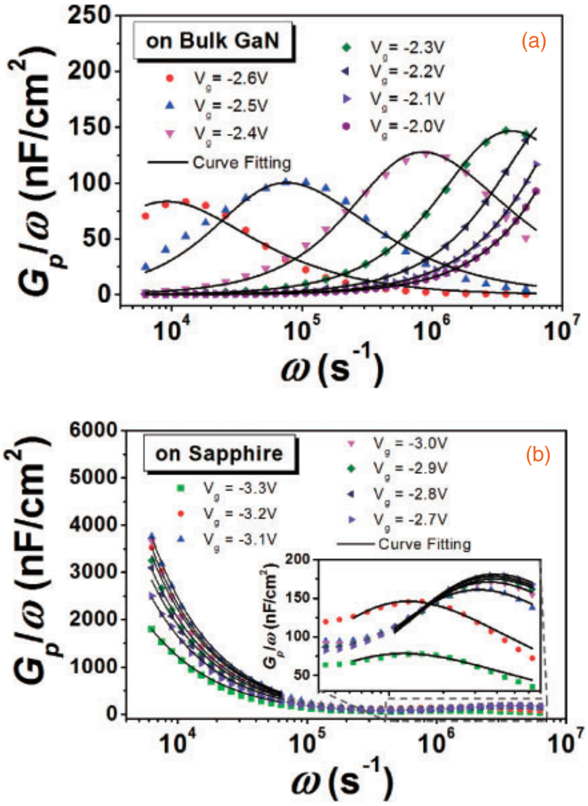

Fig. 5. Frequency-dependent parallel conductance as a function of radial frequency for the L-SBDs grown on the bulk GaN (a) and sapphire (b) substrates.

To further investigate the trapping effects in the AlGaN/GaN L-SBDs, we performed a frequency-dependent conductance analysis in the frequency range from 1 kHz to 1 MHz for both samples.[22] Figure 5 shows the plots of parallel conductance (G_p/ω) as a function of radial frequency (ω) for selected gate voltages near the threshold voltage between the two L-SBDs. Two different types of trap states with short and long time constants, designated as "fast" and "slow" trap states, respectively, were identified for the L-SBD grown on the sapphire substrate [in Fig. 5(b)], while only fast trap states could be observed in the L-SBD on the bulk GaN substrate [in Fig. 5(a)]. The fast trap states in both L-SBDs exhibited similar low densities of $(1–4) \times 10^{12}$ $cm^{-2}\,eV^{-1}$ and their time constants were in the range

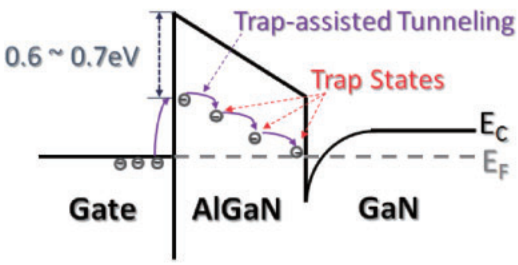

Fig. 6. Schematic energy band diagram showing the proposed leakage path through a trap-assisted tunneling mechanism in the AlGaN/GaN L-SBDs.

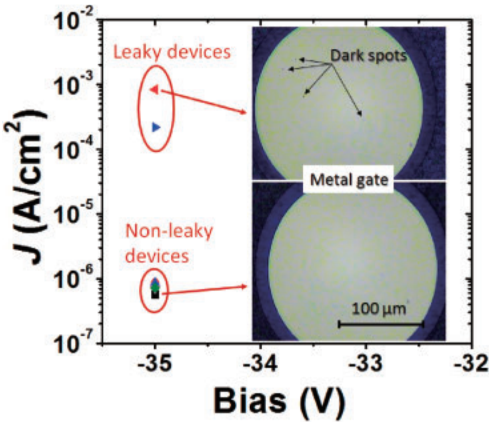

Fig. 7. Leakage current densities of the L-SBDs grown on the bulk GaN substrate in defected and normal areas with a gate bias of −35 V. The inset shows the microscopy images of the metal gate for the leaky and nonleaky devices.

between 0.05 and 200 µs. However, the densities of the slow trap states found in the L-SBD on the sapphire substrate were as high as $\sim 1 \times 10^{16}\,cm^{-2}\,eV^{-1}$ and the time constants were relatively long, in the range of 0.04–4 s. The energy level of the slow trap states was deduced to be 0.6–0.7 eV below the conduction band according to the Shockley–Read–Hall statistics. The trap states, which are considered to result from the dislocations and nitrogen vacancies, could be located both within the AlGaN barrier and at the heterojunction interface.[11] These high-density trap states could be the major cause of the high reverse leakage current in the L-SBD grown on the sapphire substrate, which provides a path for electron transport from the metal gate to the AlGaN barrier layer through a trap-assisted tunneling mechanism, as schematically shown in Fig. 6. However, such a leakage path in the L-SBD grown on the bulk GaN substrate has been significantly suppressed owing to the absence of high-density slow trap states. Thus, the very low reverse leakage current was experimentally obtained.

Nevertheless, the defect/dislocation density of the epistructure could not be totally uniform across the whole sample even using a bulk GaN substrate. Some devices with a high reverse leakage current density of $\sim 10^{-3}\,A/cm^2$ were found at the defected area of the sample grown on the bulk GaN substrate. Under the microscope, some dark spots could be observed on the metal gate of the leaky devices, while they did not appear for the nonleaky ones with very low leakage currents, as shown in Fig. 7. We suspect that those dark spots could result from the surface defects and were one of the culprits for the relatively high leakage current. This result could, in turn, be evidence of the correlation of defects with device leakage current.

In summary, on a bulk GaN substrate, we grew and fabricated an AlGaN/GaN L-SBD showing ultralow reverse leakage current density below $10^{-6}\,A/cm^2$, which was over 4 orders of magnitude lower than that of the reference L-SBD grown on the sapphire substrate. Owing to the high crystalline quality and good surface morphology achieved by homoepitaxy, the high-density slow trap states were not found in the L-SBD grown on the bulk GaN substrate. As a result, the leakage path through the trap-assisted tunneling mechanism was significantly suppressed.

Acknowledgments This work was supported in part by the Research Grants Council (RGC) theme-based research scheme (TRS) of the Hong Kong Special Administrative Region Government under Grant No. T23-612/12-R and in part by the National Natural Science Foundation of China under Grant No. 51507131. The authors would like to thank the staff of NFF and MCPF of HKUST for technical support.

1) W. J. Ha, S. Chhajed, S. J. Oh, S. Hwang, J. K. Kim, J.-H. Lee, and K.-S. Kim, Appl. Phys. Lett. **100**, 132104 (2012).
2) R. Chu, L. Shen, N. Fichtenbaum, D. Brown, C. Zhen, S. Keller, S. P. DenBaars, and U. K. Mishra, IEEE Electron Device Lett. **29**, 974 (2008).
3) J. W. Chung, J. C. Roberts, E. L. Piner, and T. Palacios, IEEE Electron Device Lett. **29**, 1196 (2008).
4) J. Kotani, M. Kaneko, H. Hasegawa, and T. Hashizume, J. Vac. Sci. Technol. B **24**, 2148 (2006).
5) N. Lee, M. Lee, W. Choi, D. Kim, N. Jeon, S. Choi, and K. Seo, Jpn. J. Appl. Phys. **53**, 04EF10 (2014).
6) M.-W. Ha, H. Woo, C. H. Roh, C.-K. Hahn, O. Seok, and M.-K. Han, 25th Int. Vacuum Nanoelectronics Conf. (IVNC), 2012, p. 1.
7) Y.-S. Lin, Y.-W. Lain, and S. S. H. Hsu, IEEE Electron Device Lett. **31**, 102 (2010).
8) L. Liu, Y. Xi, S. Ahn, F. Ren, B. P. Gila, S. J. Pearton, and I. I. Kravchenko, J. Vac. Sci. Technol. B **32**, 052201 (2014).
9) E. T. Yu, X. Z. Dang, L. S. Yu, D. Qiao, P. M. Asbeck, S. S. Lau, G. J. Sullivan, K. S. Boutros, and J. M. Redwing, Appl. Phys. Lett. **73**, 1880 (1998).
10) E. Matioli, B. Lu, and T. Palacios, IEEE Trans. Electron Devices **60**, 3365 (2013).
11) S. Saadaoui, M. M. B. Salem, M. Gassoumi, H. Maaref, and C. Gaquière, J. Appl. Phys. **110**, 013701 (2011).
12) P. K. Rao, B. Park, S. Lee, Y. Noh, M. Kim, and J. Oh, J. Appl. Phys. **110**, 013716 (2011).
13) S. Huang, B. Shen, F. Xu, F. Lin, Z. Miao, J. Song, L. Lu, L. Cen, L. Sang, Z. Qin, Z. Yang, and G. Zhang, Semicond. Sci. Technol. **24**, 055005 (2009).
14) T. Tanabe, S. Hashimoto, Y. Yoshizumi, and M. Kiyama, SEI Tech. Rev. **64** (April 2007).
15) P. Kruszewski, P. Prystawko, I. Kasalynas, A. Nowakowska-Siwinska, M. Krysko, J. Plesiewicz, J. Smalc-Koziorowska, R. Dwilinski, M. Zajac, R. Kucharski, and M. Leszczynski, Semicond. Sci. Technol. **29**, 075004 (2014).
16) E. Bahat-Treidel, O. Hilt, R. Zhytnytska, A. Wentzel, C. Meliani, J. Wurfl, and G. Trankle, IEEE Electron Device Lett. **33**, 357 (2012).
17) J. Lee, C. Park, K. Im, and J. Lee, IEEE Trans. Electron Devices **60**, 3032 (2013).
18) C. H. Chen, S. M. Baier, D. K. Arch, and M. S. Shur, IEEE Trans. Electron Devices **35**, 570 (1988).
19) Y. Lv, Z. Lin, T. D. Corrigan, J. Zhao, Z. Cao, L. Meng, C. Luan, Z. Wang, and H. Chen, J. Appl. Phys. **109**, 074512 (2011).
20) L. Geng, F. A. Ponce, S. Tanaka, H. Omiya, and Y. Nakagawa, Phys. Status Solidi A **188**, 803 (2001).
21) F. Roccaforte, F. Giannazzo, F. Iucolano, J. Eriksson, M. H. Weng, and V. Raineri, Appl. Surf. Sci. **256**, 5727 (2010).
22) R. Stoklas, D. Gregušová, J. Novák, A. Vescan, and P. Kordoš, Appl. Phys. Lett. **93**, 124103 (2008).